Chinese Chemical Letters 35 (2024) 108827

Contents lists available at ScienceDirect

Chinese Chemical Letters

journal homepage: www.elsevier.com/locate/cclet

# Design, synthesis, and biological evaluation of benzo[4,5]thieno[2,3-*d*]pyrimidine derivatives as novel HIV-1 NNRTIs

Bairu Meng[a], Zongji Zhuo[a], Han Yu[a], Sining Tao[a], Zixuan Chen[a], Erik De Clercq[b], Christophe Pannecouque[b], Dongwei Kang[a,c,*], Peng Zhan[a,c,*], Xinyong Liu[a,c,*]

[a] *Department of Medicinal Chemistry, Key Laboratory of Chemical Biology (Ministry of Education), School of Pharmaceutical Sciences, Cheeloo College of Medicine, Shandong University, Ji'nan 250012, China*
[b] *Laboratory of Virology and Chemotherapy, Rega Institute for Medical Research, K.U. Leuven, Leuven B-3000, Belgium*
[c] *China-Belgium Collaborative Research Center for Innovative Antiviral Drugs of Shandong Province, Ji'nan 250012, China*

ARTICLE INFO

*Article history:*
Received 7 June 2023
Revised 18 July 2023
Accepted 19 July 2023
Available online 24 July 2023

*Keywords:*
HIV-1
NNRTIs
DAPYs
Tolerant region II
Drug design

ABSTRACT

Inspired by our previous studies to discover novel human immunodeficiency virus-1 (HIV-1) non-nucleoside reverse transcriptase inhibitors (NNRTIs) by targeting the tolerant region II of the NNRTIs binding pocket (NNIBP), a series of novel benzo[4,5]thieno[2,3-*d*]pyrimidine derivatives were designed through structure-based drug design as novel potent HIV-1 NNRTIs. The results showed that compound **16b** was the most active inhibitor, exhibiting 50% effective concentration ($EC_{50}$) values from 0.021 μmol/L to 0.298 μmol/L against wild-type (WT) and a panel of NNRTIs-resistant HIV-1 strains. Moreover, **16b** was demonstrated with a significantly low 50% cytotoxicity concentration ($CC_{50}$) value (>200 μmol/L) and high selectivity index (SI) values. In addition, **16b** yielded moderate reverse transcriptase (RT) enzyme inhibition with a 50% inhibition concentration ($IC_{50}$) value of 0.183 μmol/L, which demonstrated that it acted as HIV-1 NNRTIs. The binding mode of **16b** with RT was also illustrated *via* molecular docking. Overall, this work provided a novel lead compound for developing potent HIV-1 NNRTIs.

© 2024 Published by Elsevier B.V. on behalf of Chinese Chemical Society and Institute of Materia Medica, Chinese Academy of Medical Sciences.

The acquired immune deficiency syndrome (AIDS), a malignant infectious disease caused by human immunodeficiency virus (HIV), has affected nearly 38.4 million patients with 0.65 million deaths at the end of 2021 [1]. HIV is a member of the Retroviridae family and includes two subtypes: HIV-1 and HIV-2. Between them, HIV-1 is the main causative agent of AIDS on account of its higher infectivity and pathogenicity [2]. During the HIV-1 replication cycle, reverse transcriptase (RT) is responsible for the conversion of the viral single-stranded RNA into double-stranded proviral DNA [3]. Without RT, replication is impaired and the viral life cycle is shut down [4,5]. Thus, RT has garnered significant attention and RT inhibitors are key components of the highly active antiretroviral therapy (HARRT) regimen [6]. Currently, there are two types of RT inhibitors, including nucleoside RT inhibitors (NRTIs) which are incorporated into the elongating viral DNA and prevent further elongation of the growing DNA strand and non-nucleoside RT inhibitors (NNRTIs) which bind to an allosteric pocket (NNRTI-binding pocket, NNIBP) near but distinct from the active site to inhibit RT functional status [7]. NNRTIs have shown promising selectivity and drug-like properties in contrast to NRTIs [8–12]. Up to now, six HIV-1 NNRTIs drugs have been approved by U.S. Food and Drug Administration (FDA), including the first-generation drugs delavirdine (DLV), nevirapine (NVP), and efavirenz (EFV) and the second-generation drugs etravirine (ETR), rilpivirine (RPV), and doravirine (DOR) [13]. Moreover, dapivirine (DPV, TMC120) was approved by the European Medicines Agency for marketing in 2020 [14]. However, the single mutants K103N and Y181C seriously reduced the effectiveness of the first-generation NNRTIs [15,16]. Although the second-generation NNRTIs displayed improved activity against these single mutants, adverse effects and the newly emerging single mutation (E138K) and double mutation RES056 (K103N + Y181C) severely limited their clinical application [17]. Therefore, there is an urgent need to discover new generation of drugs with more effective activity and safety profiles.

With ETR as the lead compound, series of novel potent HIV-1 NNRTIs have been identified in our lab, such as 2,4,5-trisubstituted pyrimidine derivative **3** [18], piperidine-substituted thiophene[2,3-*d*]pyrimidine derivative **4** [19] and fluorine-substituted diarylthiophene[3,2-*d*]pyrimidine derivative **5** (Fig. 1) [20]. Among them,

* Corresponding authors.
*E-mail addresses:* kangdongwei@126.com (D. Kang), zhanpeng1982@sdu.edu.cn (P. Zhan), xinyongl@sdu.edu.cn (X. Liu).

https://doi.org/10.1016/j.cclet.2023.108827
1001-8417/© 2024 Published by Elsevier B.V. on behalf of Chinese Chemical Society and Institute of Materia Medica, Chinese Academy of Medical Sciences.

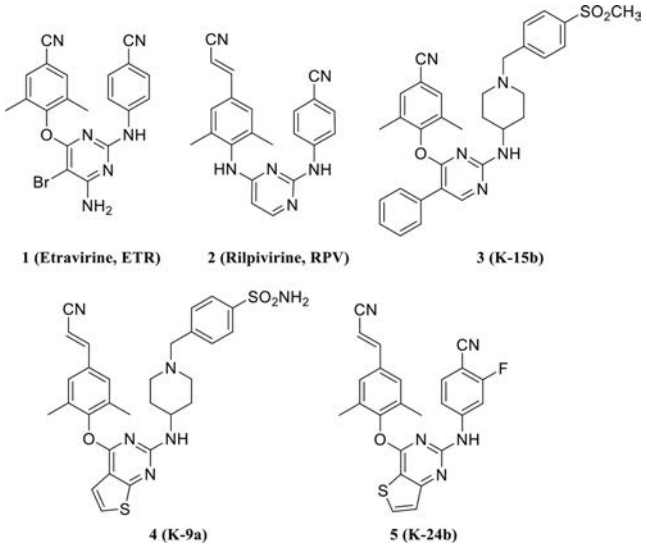


**Fig. 1.** Chemical structures of ETR, RPV and our previously reported NNRTIs **3**, **4**, and **5**.

**4** and **5** were demonstrated with highly potent antiviral activity and improved resistance profiles against HIV-1 wild-type (WT) and a panel of NNRTIs-resistant strains. Although **3** showed an outstanding activity against HIV-1 WT with a 50% effective concentration ($EC_{50}$) value of 4.93 nmol/L, its potency toward the most common double-mutant strain RES056 ($EC_{50} = 590$ nmol/L) sharply decreased. The conformational superposition analysis of **3** and **4** with RT indicated that they adopted a similar horseshoe-like conformation in the NNIBP. The binding modes of **4** illustrated that the S atom of thiophene[2,3-*d*]pyrimidine scaffold was involved in a hydrogen-bond with the backbone of Lys101 through a bridging water molecule, which were believed to play a crucial role in improving resistance to drug resistance. In the case of compound **3**, its phenyl group which linked to the $C_5$ position of the central

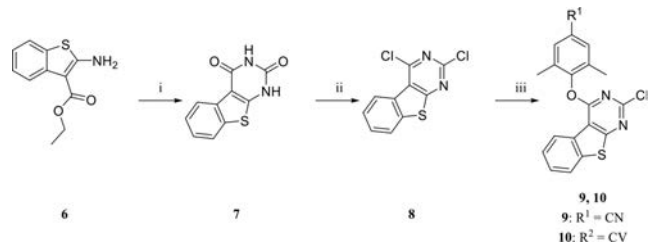


**Scheme 1.** Synthesis of **9** and **10**. Reagents and conditions: (i) urea, microwave reaction, 200 °C; (ii) $POCl_3$, 110 °C; (iii) $K_2CO_3$, DMF, r.t.

pyrimidines can point to the tolerant region II of NNIBP, but it did not develop any interactions with NNIBP. Therefore, given the results obtained from our previous explorations, it was still worth further exploring the elaborated structural modifications of central core.

The binding modes of **3** and **4** with WT HIV-1 RT revealed that the central pyrimidine fit in the same site and the thienyl substitution of **4** blocked in between the 5-phenylpyrimidine of **3**, suggesting that we could merge the two central cores into the benzo[4,5]thieno[2,3-*d*]pyrimidine (Fig. 2). We hope the newly introduced central core could establish more effective interactions with Lys101 to exhibit improved drug resistance profiles and get a deeper insight of the structure–activity relationships (SARs) of the NNIBP tolerant region II. Additionally, the privileged left wings of **3** and **4** were kept in this work. Meanwhile, the cyanophenyl groups and piperidine-linked aryl structures in the right wing of **4** and **5** were introduced to the benzo[4,5]thieno[2,3-*d*]pyrimidine scaffold *via* molecular hybridization and bioisosterism strategies. A totally of 14 novel derivatives were designed, synthesized and performed their biological evaluation in this work.

As depicted in Scheme 1, ethyl 2-aminobenzo[*b*]thiophene-3-carboxylate and urea were used as the starting materials to synthesis intermediate **7** *via* microwave reaction at 200 °C, and intermediate **7** was subsequently treated with $POCl_3$ to yield

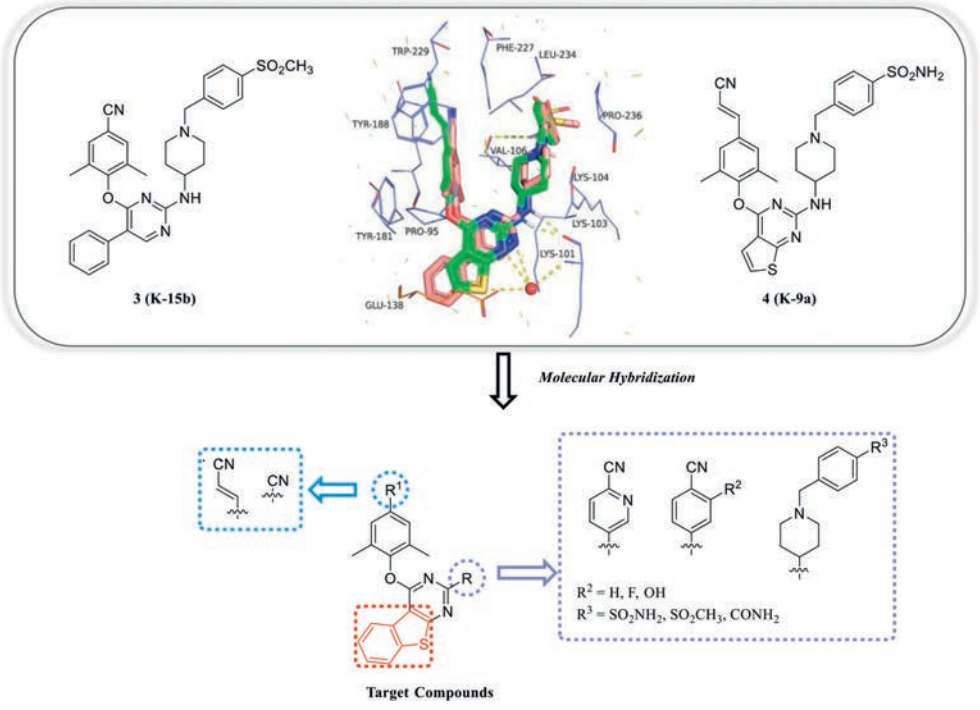


**Fig. 2.** Design of the novel benzo[4,5]thieno[2,3-*d*]pyrimidine derivatives.

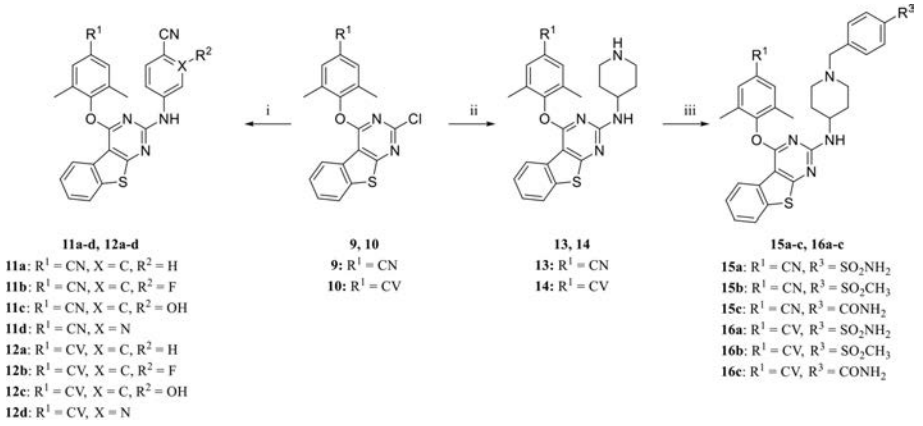


**Scheme 2.** Synthesis of **11a–d**, **12a–d**, **15a–c** and **16a–c**. Reagents and conditions: (i) BINAP, $PdCl_2(PPh_3)_2$, $Cs_2CO_3$, 1,4-dioxane, 120 °C; (ii) $K_2CO_3$, DMF, reflux; then TFA, DCM, r.t.; (iii) substituted benzyl chloride (or bromide), $K_2CO_3$, DMF, r.t.

the central benzo[4,5]thieno[2,3-*d*]pyrimidine scaffold **8**. Compound **9** was obtained by substitution reaction of **8** with 4–hydroxy–3,5-dimethylbenzonitrile in the presence of potassium carbonate ($K_2CO_3$) in dimethylformamide (DMF) at room temperature (r.t.). Likewise, **8** was reacted with (*E*)−3-(4–hydroxy–3,5-dimethylphenyl)acrylonitrile to afford intermediate **10**.

As depicted in Scheme 2, Pd-catalyzed Buchwald-Hartwig coupling of **9** or **10** with various cyano aromatic amines yielded **11a–d** and **12a–d**. Compound **9** or **10** was treated with *N*-(*tert*–butoxycarbonyl)−4-amino-piperidine and subsequent deprotection delivered **13** or **14** using trifluoroacetic acid (TFA), which was reacted with substituted benzyl chloride (or bromide) to give the target compounds **15a–c** and **16a–c**. Detailed procedures and compound characterizations can be found in Supporting information.

All the newly synthesized compounds were evaluated for their biological activity to WT HIV-1 IIIB strain and a double-mutant HIV-1 strain RES056 (K103N/Y181C) in MT-4 cells with the MTT method. The selected potent inhibitors were tested for their activity against other common NNRTIs-resistant strains, including L100I, K103N, Y181C, Y188L, E138K, and F227L/V106A. NVP, ETR, and EFV were acted as reference drugs. Experimental procedure can be found in Supporting information. The values of $EC_{50}$ (anti-HIV-1 potency), 50% cytotoxicity concentration ($CC_{50}$), selectivity index (SI, $CC_{50}/EC_{50}$ ratio) of these novel inhibitors were determined and shown in Tables 1 and 2.

As depicted in Table 1, most compounds exhibited promising potency against HIV-1 IIIB with $EC_{50}$ values of 0.021 μmol/L to 0.100 μmol/L. Of special note is that **16b** with the $-SO_2CH_3$ group showed the highest activity against HIV-1 IIIB ($EC_{50} = 0.021$ μmol/L) and outstanding activity against RES056 ($EC_{50} = 0.298$ μmol/L). Although **16b** displayed slightly inferior antiviral activities compared to ETR ($EC_{50\ IIIB} = 0.003$ μmol/L, $EC_{50\ RES056} = 0.083$ μmol/L), it demonstrated much reduced cytotoxicity ($CC_{50}$ > 200 μmol/L) and higher SI values ($SI_{IIIB}$ > 9419, $SI_{RES056}$ > 672) than that of ETR ($CC_{50}$ > 4.59 μmol/L, $SI_{IIIB}$ > 1633, $SI_{RES056}$ > 55). Replacing the $-SO_2CH_3$ group in the $R^2$ position of **16b** with $-SO_2NH_2$ group and $-CO_2NH_2$ group resulted in compounds **16a** and **16c**, which showed promising activity against HIV-1 IIIB ($EC_{50} = 0.027$ and 0.100 μmol/L, respectively). Interestingly, changing piperidine-linked substituted benzene groups to the cyano aromatic amines of **12a**, **12b**, and **12d** ($EC_{50\ IIIB} = 0.023$–$0.085$ μmol/L, $EC_{50\ RES056} = 0.565$–$0.960$ μmol/L) also showed considerable activity against HIV-1 IIIB but all of their potencies against RES056 still did not exceed **16b** and ETR. Particularly, **12d** ($EC_{50\ IIIB} = 0.023$ μmol/L, $EC_{50\ RES056} = 0.894$ μmol/L) exhibited comparable activity against HIV-1 IIIB but inferior activity against RES056, being comparable to that of ETR. However, **12c** was devoid of activity against HIV-1 IIIB and RES056, suggesting that cyano aromatic structure with a 2–hydroxy group in the right wing had an adverse effect on the potency of compounds against a panel of NNRTI-resistant strains. When replacing the cyanovinyl substituent with cyano substituent on the left wing, several compounds **11a** ($EC_{50} = 0.041$ μmol/L), **15a** ($EC_{50} = 0.030$ μmol/L) and **15b** ($EC_{50} = 0.035$ μmol/L) retained potency against HIV-1 IIIB. But they showed inferior potency against RES056, declaring that cyanovinyl substituent was important to improve resistance profiles.

Additionally, **11a**, **12a**, **12d**, **15a**, **15b**, **16a** and **16b** were selected to performed their antiviral potency against a panel of single mutant HIV-1 strains, including L100I, K103N, Y181C, Y188L, E138K, and double mutant strain F227L + V106A. As shown in Table 2, the most potent RES056 inhibitor **16b** could strongly inhibit these mutant strains, with $EC_{50}$ values of 0.027 μmol/L (L100I), 0.017 μmol/L (K103N), 0.085 μmol/L (Y181C), 0.121 μmol/L (Y188L), 0.112 μmol/L (E138K), and 0.041 μmol/L (F227L + V106A). In addition, **16a** also showed potent inhibitory activity against L100I ($EC_{50} = 0.029$ μmol/L), K103N ($EC_{50} = 0.026$ μmol/L), and F227L + V106A ($EC_{50} = 0.043$ μmol/L), while showing weak activity against Y181C ($EC_{50} = 0.119$ μmol/L), Y188L ($EC_{50} = 0.121$ μmol/L), and E138K ($EC_{50} = 0.175$ μmol/L). These results demonstrated that the structure of the cyano-group on the left and the aminopyridine on the right was more conducive to the improvement of the activity of the compound against the mutant strains, and compound **16b** with these two structural features exhibited the optimal resistance to drug resistance.

The ability of representative compounds to inhibit recombinant WT HIV-1 RT enzyme were measured *in vitro* to confirm the binding target of these novel inhibitors. NVP and ETR were chosen as the reference drugs in this assay. Detailed procedures can be found in Supporting information. As depicted in Table 3, these compounds exhibited significant binding-affinity to WT HIV-1 RT ($IC_{50} = 0.099$–$0.366$ μmol/L), being about 3−10-fold potent than that of NVP ($IC_{50} = 1.02$ μmol/L). Although these novel inhibitors exhibited inferior activities compared to that of ETR ($IC_{50} = 0.011$ μmol/L), these results could validate that the binding target of the newly designed compounds was HIV-1 RT.

To elucidate the contribution of the 2,4-bisubstituted benzo[4,5]thieno[2,3-*d*]pyrimidine motif in **16b** binding to WT HIV-1 RT (from PDB ID: 6C0N) and RES056 HIV-1 RT (from PDB ID: 6C0R), molecular docking study was performed with Maestro (Maestro, Schrödinger, LLC, New York, NY, 2019). The docking results were visualized by PyMOL. Detailed procedures can be found in Supporting information. As shown in Fig. 3, **16b** adopted

**Table 1**
Antiviral potency against HIV-1 IIIB and RES056, cytotoxicity, and SI values of target compounds **11a–d**, **12a–d**, **15a–c** and **16a–c**.

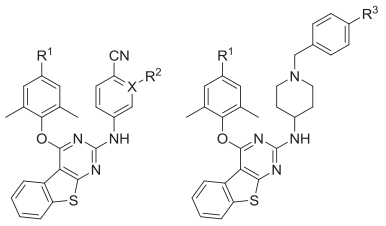


| Compd. | $R^1$ | X | $R^2$ | $R^3$ | $EC_{50}$ (μmol/L) [a] | | $CC_{50}$ (μmol/L) [b] | SI [c] | |
|---|---|---|---|---|---|---|---|---|---|
| | | | | | IIIB | RES056 | | IIIB | RES056 |
| **11a** | CN | C | H | – | 0.041 ± 0.014 | 2.60 ± 2.16 | >279 | >6767 | >107 |
| **11b** | CN | C | F | – | >179 | – | >179 | <1 | – |
| **11c** | CN | C | OH | – | 1.05 ± 0.417 | >28.3 | 28.3 ± 4.42 | 27 | <1 |
| **11d** | CN | N | – | – | 0.306 ± 0.099 | >29.0 | 29.0 ± 3.34 | 95 | <1 |
| **12a** | CV | C | H | – | 0.050 ± 0.019 | 0.565 ± 0.310 | 236 ± 5.73 | 4701 | 419 |
| **12b** | CV | C | F | – | 0.085 ± 0.039 | 0.960 ± 0.138 | >254 | >3003 | >265 |
| **12c** | CV | C | OH | – | 0.285 ± 0.072 | >41.0 | 40.9 ± 11.3 | 144 | <1 |
| **12d** | CV | N | – | – | 0.023 ± 0.016 | 0.894 ± 0.370 | >263 | >11,329 | >295 |
| **15a** | CN | – | – | $SO_2NH_2$ | 0.030 ± 0.007 | 0.981 ± 0.208 | 18.7 ± 3.92 | 636 | 19 |
| **15b** | CN | – | – | $SO_2CH_3$ | 0.035 ± 0.009 | 1.84 ± 0.377 | 21.9 ± 6.35 | 631 | 12 |
| **15c** | CN | – | – | $CONH_2$ | >9.22 | – | >9.22 | <1 | |
| **16a** | CV | – | – | $SO_2NH_2$ | 0.027 ± 0.008 | 0.226 ± 0.017 | 21.2 ± 3.27 | 803 | 94 |
| **16b** | CV | – | – | $SO_2CH_3$ | 0.021 ± 0.004 | 0.298 ± 0.190 | >200 | >9419 | >672 |
| **16c** | CV | – | – | $CONH_2$ | 0.100 ± 0.064 | 2.23 ± 0.956 | 23.8 ± 7.15 | 238 | 11 |
| NVP | – | – | – | – | 0.083 ± 0.025 | >9.51 | >9.51 | >115 | – |
| ETR | – | – | – | – | 0.003 ± 0.001 | 0.083 ± 0.021 | >4.59 | >1633 | >55 |
| EFV | – | – | – | – | 0.003 ± 0.001 | 0.492 ± 0.150 | >6.34 | >1860 | >13 |

[a] $EC_{50}$: concentration of compound required to achieve 50% protection of MT-4 cell cultures against HIV-1-induced cytopathicity, as determined by the MTT method.
[b] $CC_{50}$: concentration required to reduce the viability of mock-infected cell cultures by 50%, as determined by the MTT method.
[c] SI: selectivity index, the ratio of $CC_{50}/EC_{50}$.

**Table 2**
Antiviral potency against mutant HIV-1 strains of target compounds **11a**, **12a**, **12d**, **15a**, **15b**, **16a** and **16b**.

| Compd. | $EC_{50}$ (μmol/L) [a] | | | | | |
|---|---|---|---|---|---|---|
| | L100I | K103N | Y181C | Y188L | E138K | F227L + V106A |
| **11a** | 0.179 ± 0.045 | 0.032 ± 0.011 | 0.265 ± 0.081 | 0.132 ± 0.023 | 0.050 ± 0.014 | 0.394 ± 0.177 |
| **12a** | 0.049 ± 0.012 | 0.044 ± 0.011 | 0.292 ± 0.062 | 0.232 ± 0.075 | 0.252 ± 0.127 | 0.565 ± 0.310 |
| **12d** | 0.043 ± 0.017 | 0.031 ± 0.019 | 0.114 ± 0.069 | 0.153 ± 0.050 | 0.060 ± 0.169 | 0.484 ± 0.115 |
| **15a** | 0.178 ± 0.048 | 0.030 ± 0.003 | 0.136 ± 0.048 | 0.107 ± 0.017 | 0.097 ± 0.026 | 0.132 ± 0.095 |
| **15b** | 0.181 ± 0.041 | 0.056 ± 0.010 | 0.233 ± 0.038 | 0.203 ± 0.049 | 0.190 ± 0.072 | 0.301 ± 0.251 |
| **16a** | 0.029 ± 0.003 | 0.026 ± 0.007 | 0.119 ± 0.042 | 0.121 ± 0.039 | 0.175 ± 0.051 | 0.043 ± 0.009 |
| **16b** | 0.027 ± 0.002 | 0.017 ± 0.002 | 0.085 ± 0.005 | 0.121 ± 0.066 | 0.112 ± 0.048 | 0.041 ± 0.020 |
| NVP | 1.18 ± 0.811 | 5.26 ± 2.26 | >9.51 | >9.51 | 0.064 ± 0.024 | >9.51 |
| ETR | 0.008 ± 0.003 | 0.003 ± 0.001 | 0.018 ± 0.006 | 0.022 ± 0.006 | 0.011 ± 0.002 | 0.018 ± 0.012 |
| EFV | 0.065 ± 0.068 | 0.077 ± 0.023 | 0.006 ± 0.002 | 0.353 ± 0.195 | 0.005 ± 0.001 | 0.460 ± 0.539 |

[a] $EC_{50}$: concentration of compound required to achieve 50% protection of MT-4 cell cultures against HIV-1-induced cytopathicity, as determined by the MTT method.

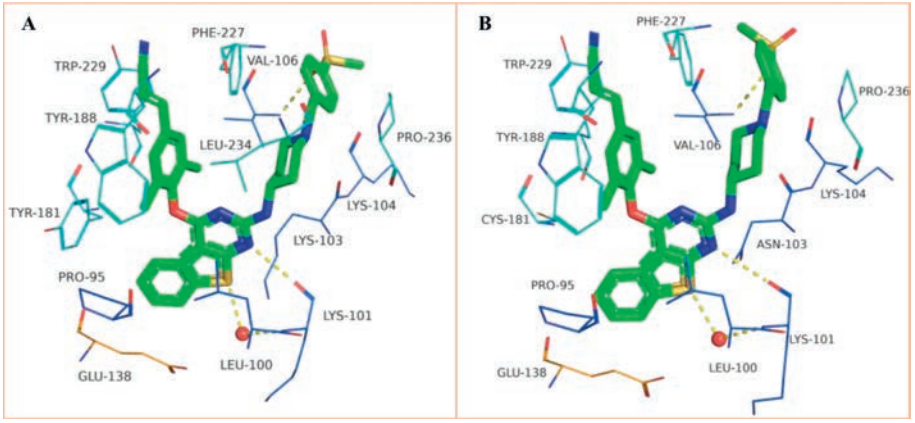


**Fig. 3.** Predicted binding modes of **16b** with the HIV-1 WT RT (A, PDB code: 6C0N) and RES056 HIV-1 RT (B, PDB code: 6C0R).

**Table 3**
Inhibitory activity against WT HIV-1 RT of target compounds **11a**, **12a**, **12d**, **15a**, **15b**, **16a** and **16b**.

| Compd. | $IC_{50}$ (μmol/L) [a] | Compd. | $IC_{50}$ (μmol/L) [a] |
|---|---|---|---|
| **11a** | 0.115 ± 0.0079 | **16a** | 0.259 ± 0.0679 |
| **12a** | 0.099 ± 0.000 | **16b** | 0.183 ± 0.0612 |
| **12d** | 0.130 ± 0.001 | NVP | 1.02 ± 0.37 |
| **15a** | 0.211 ± 0.000 | ETR [b] | 0.011 ± 0.000 |
| **15b** | 0.366 ± 0.038 | | |

[a] $IC_{50}$: inhibitory concentration required to inhibit biotin deoxyuridine triphosphate incorporation into WT HIV-1 RT by 50%.
[b] Results from Ref. [21].

a horseshoe conformation in the NNIBP consistent with classical DAPY derivatives. Concretely, the docking results maintained the identify of our previous investigations and could be described as follows: (1) Benzothiophene group of the central core sat in the tolerant region II of NNIBP as envisioned and the thiophene S atom formed a hydrogen bond with Lys101 through a bridging water molecule, which provided great benefits to inhibit RT and the N atom of the pyrimidine also formed a hydrogen bond with the backbone of Lys101; (2) The left wing fully occupied the hydrophobic sub-pocket and developed stronger hydrophobic interactions with Phe227 and Trp229; (3) The right wing also showed similar interactions with Val106 as in other RT/DAPY structures. It was worth mentioning that **16b** lost essential water-mediated hydrogen bonds with Lys101, making it reduced potency that of **3** and **4**.

We next predicted the binding mode of **16b** with RES056 RT. Due to the flexibility of the right wing of **16b**, the K103N mutation did not affect resistance profiles. However, the mutation of Tyr181 residue (Y181C) locating in the hydrophobic tunnel had an adverse effect on the hydrophobic interactions between left wing and Tyr181. The molecular planarity of the fused benzo[4,5]thieno[2,3-*d*]pyrimidine scaffold may also account for the decreased resistance profiles of **16b**.

In the current study, we leverage our understanding of the HIV-1 RT inhibition mechanism based on the binding modes of HIV-1 RT with two inhibitors to guide the lead optimization. Based on the superposition analysis of co-crystal structures, the central cores of **3** and **4** were merged into the benzo[4,5]thieno[2,3-*d*]pyrimidine to improve compounds' antiviral activity against WT and mutant HIV-1 strains. The results demonstrated that **16b** exhibited the most potent activity against HIV-1 WT strain and NNRTIs-resistant strains ($EC_{50} = 0.017–0.298$ μmol/L). Moreover, it also showed significant low cytotoxicity ($CC_{50} > 200$ μmol/L) and high SI values. The enzymatic inhibitory activity ($IC_{50} = 0.183$ μmol/L) results proved the target of these novel compounds were HIV-1 RT. The docking results verified that the N atom and S atom of the central core could form double hydrogen bonds with the backbone of Lys101, which were in agreement with our expectation. Taken together, **16b** was a novel HIV-1 RT inhibitor that displayed potent antiviral activity and thus had promising potential for further study.

## Declaration of competing interest

The authors declare that they have no known competing financial interests or personal relationships that could have appeared to influence the work reported in this paper.

## Acknowledgments

We gratefully acknowledge financial support from the National Natural Science Foundation of China (NSFC, Nos. 81973181, 82273773), Shandong Provincial Natural Science Foundation (Nos. ZR2020YQ61, ZR2020JQ31), Qilu Young Scholars Program of Shandong University and Taishan Scholar Program at Shandong Province. The technical assistance of Mr. Kris Uyttersprot and Mrs. Kristien Erven, for the HIV experiments is gratefully acknowledged.

## Supplementary materials

Supplementary material associated with this article can be found, in the online version, at doi:10.1016/j.cclet.2023.108827.

## References

[1] HIV data and statistics. https://www.who.int/teams/global-hiv-hepatitis-and-stis-programmes/hiv/strategic-information/hiv-data-and-statistics (2023) (accessed 2022-11-17).
[2] A.S. Fauci, H.C. Lane, N. Engl. J. Med. 383 (2020) 1–4.
[3] G. Bec, B. Meyer, M.A. Gerard, et al., J. Am. Chem. Soc. 135 (2013) 9743–9752.
[4] A. Tavassoli, Chem. Soc. Rev. 40 (2011) 1337–1346.
[5] C. Flexner, Nat. Rev. Drug Discov. 6 (2007) 959–966.
[6] R.J. Shattock, M. Warren, S. McCormack, C.A. Hankins, Science 333 (2011) 42–43.
[7] D. Li, P. Zhan, E. De Clercq, X. Liu, J. Med. Chem. 55 (2012) 3595–3613.
[8] D. Feng, F. Wei, Y. Sun, et al., Chin. Chem. Lett. 32 (2021) 4053–4057.
[9] D. Feng, H. Lin, L. Jiang, et al., Eur. J. Med. Chem. 246 (2023) 114957.
[10] F. Zhao, H. Zhang, M. Xie, et al., J. Med. Chem. 66 (2023) 2102–2115.
[11] Z. Wang, D. Kang, D. Feng, et al., Eur. J. Med. Chem. 206 (2020) 112811.
[12] S. Han, Y. Lei, C. Pannecouque, et al., Chin. Chem. Lett. 31 (2020) 764–768.
[13] Z. Wang, S. Cherukupalli, M. Xie, et al., J. Med. Chem. 65 (2022) 3729–3757.
[14] N. Bhavaraju, K. Shears, K. Schwartz, et al., Curr. HIV AIDS Rep. 18 (2021) 508–517.
[15] D.A. Lehman, D.C. Wamalwa, C.O. McCoy, et al., J. Acquir. Immune. Defic. Syndr. 60 (2012) 225–233.
[16] M.E. Cilento, K.A. Kirby, S.G. Sarafianos, Chem. Rev. 121 (2021) 3271–3296.
[17] A. Olson, N. Bannert, A. Sönnerborg, et al., AIDS 32 (2018) 161–169.
[18] D. Kang, F.X. Ruiz, Y. Sun, et al., J. Med. Chem. 64 (2021) 4239–4256.
[19] D. Kang, D. Feng, Y. Sun, et al., J. Med. Chem. 63 (2020) 4837–4848.
[20] D. Kang, F.X. Ruiz, D. Feng, et al., J. Med. Chem. 63 (2020) 1298–1312.
[21] D. Kang, H. Zhang, Z. Wang, et al., J. Med. Chem. 62 (2019) 1484–1501.